α-Agostic Interactions in Cp*W(NO)(CH_2CMe_3)$_2$ and Related Nitrosyl Complexes

Robert Bau,*,† Sax A. Mason,‡ Brian O. Patrick,§ Craig S. Adams,§ W. Brett Sharp,§ and Peter Legzdins*,§

Department of Chemistry, University of Southern California, Los Angeles, California 90089, Institut Laue-Langevin, Grenoble, France F-38042, and Department of Chemistry, University of British Columbia, Vancouver, British Columbia, Canada V6T 1Z1

Received July 12, 2001

The solid-state molecular structure of Cp*W(NO)(CH_2CMe_3)$_2$ (**1**) has been shown to contain one "strongly agostic" and one "weakly agostic" methylene hydrogen atom by a neutron diffraction analysis at 120 K and by an X-ray diffraction analysis at −100 °C. The X-ray diffraction analysis of Cp*W(NO)(CH_2SiMe_3)$_2$ (**2**) at −20 °C reveals that its solid-state molecular structure possesses a crystallographically imposed mirror plane. Consequently, only the average existence of a relatively strong C−H···M interaction for each hydrocarbyl ligand in **2** in the solid state can be established. The ^{1}H and gated ^{13}C{^{1}H} NMR spectra of representative Cp′M(NO)(R)(R′) (M = Mo, W; R = hydrocarbyl, R′ = hydrocarbyl, halide, amide) complexes exhibit spectral parameters for the α-H and α-C atoms (i.e., δ_H, δ_C, $\Delta\delta_H$, ΔJ_{HC}, and J_{HW}) that provide evidence for the presence of α-agostic interactions in the molecular structures of these complexes in solution. The picture that has emerged from these investigations is that these complexes do adopt an α-agostic structure both in solution and in the solid state when secondary interactions such as π-electron donation are weak (as in Cp*W(NO)(CH_2CMe_3)Cl), competitive (as in Cp*W(NO)(CH_2CMe_3)(CH_2Ph)), or not possible (as in Cp*W(NO)(hydrocarbyl)$_2$ complexes generally). The bis(hydrocarbyl) complexes are probably stereochemically nonrigid in solution, as they appear to interconvert between the two limiting structures having one strongly agostic and one weakly agostic hydrocarbyl ligand. The neopentyl ligand forms α-agostic linkages with the metal centers in all neopentyl complexes studied, and these agostic interactions appear to be independent of the nature of the metal or the ancillary cyclopentadienyl ligand. Interestingly, the presence of these ground-state agostic interactions does not correlate with the tendency of the various compounds to undergo intramolecular α-H abstraction reactions and form reactive alkylidene complexes.

Introduction

Three-center C−H···M "agostic" interactions occur frequently in electronically unsaturated organometallic complexes.[1] In all cases, the number, strength (typically <20 kcal mol^{-1}),[2,3] and geometry of these linkages depend on the energy and disposition of the vacant metal orbitals relative to the C−H bonding orbitals and upon the steric and conformational effects imposed by the molecule.[4] While these interactions can be benign, they often have a marked effect on the chemical properties of the coordinated C−H bond and the reactivity of the molecule as a whole. For example, it is now well-established that agostic C−H binding can significantly weaken the C−H bond, thereby rendering it susceptible to a wide range of inter- and intramolecular C−H activation reactions.[5−7] In other instances, the coordinated C−H bond does not break but plays an important role in lowering the activation barrier for, and in

† University of Southern California.
‡ Institut Laue-Langevin.
§ University of British Columbia.

(1) For reviews, see: (a) Brookhart, M.; Green, M. L. H. *J. Organomet. Chem.* **1983**, *250*, 395. (b) Brookhart, M.; Green, M. L. H.; Wong, L.-L. *Prog. Inorg. Chem.* **1988**, *36*, 1. (c) Crabtree, R. H.; Hamilton, D. G. *Adv. Organomet. Chem.* **1988**, *28*, 299.

(2) (a) Cotton, F. A.; Stanislowski, A. G. *J. Am. Chem. Soc.* **1974**, *96*, 5074. (b) Brookhart, M.; Green, M. L. H.; Pardy, R. B. A. *J. Chem. Soc., Chem. Commun.* **1983**, 691. (c) Morse, P. M.; Spencer, M. D.; Wilson, S. R.; Girolami, G. S. *Organometallics* **1994**, *13*, 1646.

(3) (a) Kawamura-Kuribayashi, H.; Koga, N.; Morokuma, K. *J. Am. Chem. Soc.* **1992**, *114*, 2359. (b) Lohrenz, J. C. W.; Woo, T. K.; Ziegler, T. *J. Am. Chem. Soc.* **1995**, *117*, 12793. (c) Margl, P.; Lohrenz, J. C. W.; Ziegler, T.; Blochl, P. E. *J. Am. Chem. Soc.* **1996**, *118*, 4434.

(4) For example, see: (a) Eisenstein, O.; Jean, Y. *J. Am. Chem. Soc.* **1985**, *107*, 1177. (b) Crabtree, R. H.; Holt, E. M.; Lavin, M.; Morehouse, S. M. *Inorg. Chem.* **1985**, *24*, 1986. (c) Cooper, A. C.; Clot, E.; Huffman, J. C.; Streib, W. E.; Maseras, F.; Eisenstein, O.; Caulton, K. G. *J. Am. Chem. Soc.* **1999**, *121*, 97. (d) Tenorio, M. J.; Mereiter, K.; Puerta, M. C.; Valerga, P. *J. Am. Chem. Soc.* **2000**, *122*, 11230.

(5) (a) Vigalok, A.; Uzan, O.; Shimon, L. J. W.; Ben-David, Y.; Martin, J. M. L.; Milstein, D. *J. Am. Chem. Soc.* **1998**, *120*, 12539. (b) Kanamori, K.; Broderick, W. E.; Jordan, R. F.; Willett, R. D.; Legg, J. I. *J. Am. Chem. Soc.* **1986**, *108*, 7122.

(6) (a) Turner, H. W.; Schrock, R. R.; Fellman, J. D.; Holmes, S. J. *J. Am. Chem. Soc.* **1983**, *105*, 4942. (b) Lamanna, W.; Brookhart, M.; Humphrey, M. B. *J. Am. Chem. Soc.* **1982**, *104*, 2117. (c) Toner, A. J.; Gruendemann, S.; Clot, E.; Limbach, H. H.; Donnadieu, B.; Sabo-Etienne, S.; Chaudret, B. *J. Am. Chem. Soc.* **2000**, *122*, 6777. (d) Albeniz, A. C.; Schulte, G.; Crabtree, R. H. *Organometallics* **1992**, *11*, 242. (e) Ogasawara, M.; Saburi, M. *Organometallics* **1994**, *13*, 1911.

(7) (a) Lee, D. H.; Chen, J.; Faller, J. W.; Crabtree, R. H. *J. Chem. Soc., Chem. Commun.* **2001**, 213. (b) Schrock, R. R. *Acc. Chem. Res.* **1979**, *12*, 98. (c) Fellmann, J. D.; Schrock, R. R.; Traficante, D. D. *Organometallics* **1982**, *1*, 481. (d) Warren, T. H.; Schrock, R. R.; Davis, W. M. *J. Organomet. Chem.* **1998**, *569*, 125.

10.1021/om0106231 CCC: $20.00
Publication on Web 10/04/2001

Table 1. Crystallographic Data for the Neutron and X-ray Analyses of Complexes 1 and 2

	1		
	neutron	X-ray	2
chem formula	$C_{20}H_{37}NOW$	$C_{20}H_{37}NOW$	$C_{18}H_{37}NOSi_2W$
fw	491.35	491.35	523.52
cryst class	monoclinic	monoclinic	orthorhombic
space group	$P2_1/n$	$P2_1/n$	$Pnma$
cryst dimens (mm)	0.48 × 1.8 × 4.8	0.50 × 0.35 × 0.25	0.50 × 0.25 × 0.20
cryst color	red	red	violet
a (Å)	8.8664(3)	8.9229(3)	9.6321(8)
b (Å)	21.7233(8)	21.7707(8)	19.800(5)
c (Å)	11.2865(4)	11.3202(4)	12.513(1)
β (deg)	105.555(2)	105.566(3)	90.0
V (Å^3)	2093.8(1)	2118.4(1)	2386.4(7)
Z	4	4	4
density (g cm^{-3})	1.541	1.541	1.457
wavelength (Å)	1.535	0.710 69	0.710 69
temp (K)	120	173	253
diffractometer	ILL/D-19	Rigaku/ADSC	Rigaku/ADSC
no. of rflns collected	4557	15 735	14 788
no. of rflns used in refinement	2939	4560	2678
$R(F_o)^a$	0.055	0.025	0.026
$R_w(F_o^2)^a$	0.151	0.065	0.069
S^b	1.310	0.988	0.767

[a] $R = \sum||F_o| - |F_c||/\sum|F_o|$, $F \geq 4\sigma(F)$; $R_w = \{\sum[w(F_o^2 - F_c^2)^2]/\sum[w(F_o^2)^2]\}^{1/2}$, all data. [b] $S = \{\sum[w(F_o^2 - F_c^2)^2]/(n - p)\}^{1/2}$.

influencing the stereochemical outcome of, chemical transformations such as the polymerization of alkenes.[3,8]

We have an abiding interest in the formally 16-electron complexes Cp′M(NO)(R)(R′) (Cp′ = η^5-C_5H_5, η^5-C_5Me_5; M = W, Mo; R, R′ = hydrocarbyl), and we continue to explore their rich and diverse chemistry.[9] Early on in our explorations it occurred to us that these electronically unsaturated nitrosyl complexes could well contain intramolecular α-agostic interactions. Our preliminary structural and spectroscopic investigations of $CpW(NO)(CH_2SiMe_3)_2$ in this regard in 1988 were inconclusive and led us to state that "these C−H···M links, if they do exist, do not apparently affect the (Lewis acid) chemistry of these compounds".[10] However, we subsequently discovered that the dialkyl complexes $Cp^*W(NO)(CH_2CMe_3)_2$, $Cp^*W(NO)(CH_2CMe_3)(CH_2C_6H_5)$,[11] and $CpMo(NO)(CH_2CMe_3)_2$[12] readily undergo α-H elimination of neopentane to form the corresponding alkylidene complexes Cp′M(NO)(=CHR), a process which could be due to the presence of α-agostic interactions in the ground states of the reactant molecules. Moreover, α-agostic interactions have recently been found in the related isostructural dialkyl complexes $CpNb(=NAr)(CH_2CMe_3)_2$ (Ar = C_6H_3-2,6-^{i}Pr$_2$)[13] and $CpW(\equiv CR)(CH_2R')_2$ (R, R′ = CMe_3, 1-adamantyl).[7d]

In light of these facts, we decided to conduct a thorough structural study of a representative group of Cp′M(NO)(R)(R′) complexes to investigate α-agostic bonding within these molecules. In this contribution we present the results of our investigations, which conclusively establish the existence of up to two α-agostic bonds per molecule, depending on the nature of the R′ ligands. We also delineate how these structural features relate to the observed α-H elimination reactivity in an unexpected manner.

Experimental Section

All reactions and subsequent manipulations of air- and/or water-sensitive compounds were performed under anaerobic and anhydrous conditions under an atmosphere of prepurified dinitrogen or argon. General procedures routinely employed in these laboratories have been described in detail elsewhere.[14] Hexanes, pentane, THF, and Et_2O were distilled from Na/benzophenone ketyl under dinitrogen. Deuterated solvents were purchased from Cambridge Isotope Laboratories (all >99.9 atom % D) and then degassed and vacuum-transferred from Na/benzophenone ketyl (C_6D_6), Na (toluene-d_8), or activated 4 Å molecular sieves (CD_2Cl_2). Celite and neutral alumina I were oven-dried (>130 °C) and cooled under vacuum prior to use. Dialkylmagnesium reagents $R_2Mg{\cdot}x$(dioxane) (R = Ph, CH_2Ph, CX_2CMe_3 (X = H, D), CH_2SiMe_3, CH_2CMe_2Ph) were prepared by modified literature procedures[12,15] using 2.2 equiv of dioxane. With the exception of $Cp^*W(NO)(CH_2CMe_3)_2$ (**1**), the other complexes **2**−**10**[10,11b,16,17] were prepared according to published procedures. Table 3 lists the various complexes investigated and their numbering scheme. The complex $Cp^*W(NO)(CH_2CMe_3)(NMe_2)$ (**11**) was prepared as described below, this being a modification of the procedure used to prepare related molybdenum amide complexes.[18] Reported yields of synthetic procedures are not optimized unless specified.

Low-resolution mass spectra (EI, 70 eV, probe temperature 150 °C) were recorded by Mr. M. Lapawa and Ms. L. Madilao

(8) (a) Grubbs, R. H.; Coates, G. W. *Acc. Chem. Res.* **1996**, *29*, 85. (b) Lohrenz, J. C. W.; Buhl, M.; Weber, M.; Thiel, W. *J. Organomet. Chem.* **1999**, *592*, 11. (c) Tempel, D. J.; Johnson, L. K.; Huff, R. L.; White, P. S.; Brookhart, M. *J. Am. Chem. Soc.* **2000**, *122*, 6686. (d) Tanner, M. J.; Brookhart, M.; DeSimone, J. M. *J. Am. Chem. Soc.* **1997**, *119*, 7617. (e) Olden, C. M.; Stryker, J. M. *J. Am. Chem. Soc.* **2000**, *122*, 2784.

(9) Legzdins, P.; Veltheer, J. E. *Acc. Chem. Res.* **1993**, *26*, 41.

(10) Legzdins, P.; Rettig, S. J.; Sánchez, L. *Organometallics* **1988**, *7*, 2394.

(11) (a) Tran, E.; Legzdins, P. *J. Am. Chem. Soc.* **1997**, *119*, 5071. (b) Adams, C. S.; Legzdins, P.; Tran, E. *J. Am. Chem. Soc.* **2001**, *123*, 612.

(12) Legzdins, P.; Rettig, S. J.; Veltheer, J. E. *Organometallics* **1993**, *12*, 3575.

(13) Poole, A. D.; Williams, D. N.; Kenwright, A. M.; Gibson, V. C.; Clegg, W.; Hockless, D. C. R.; O'Neil, P. A. *Organometallics* **1993**, *12*, 2549.

(14) Legzdins, P.; Rettig, S. J.; Ross, K. J.; Batchelor, R. J.; Einstein, F. W. B. *Organometallics* **1995**, *14*, 5579.

(15) Dryden, N. H.; Legzdins, P.; Trotter, J.; Yee, V. C. *Organometallics* **1991**, *10*, 2857.

(16) Debad, J. D.; Legzdins, P.; Rettig, S. J.; Veltheer, J. E. *Organometallics* **1993**, *12*, 2714.

(17) Debad, J. D.; Legzdins, P.; Batchelor, R. J.; Einstein, F. W. B. *Organometallics* **1993**, *12*, 2094.

(18) Legzdins, P.; Veltheer, J. E.; Young, M. A.; Batchelor, R. J.; Einstein, F. W. B. *Organometallics* **1995**, *14*, 407.

Table 2. Bond Distances and Angles Involving the M−CH_2EMe_3 Fragments (E = C, Si) of the Complexes Cp*W(NO)(CH_2CMe_3)$_2$ (4), Cp*W(NO)(CH_2SiMe_3)$_2$ (5), and CpW(NO)(CH_2SiMe_3)$_2$ (2)[a]

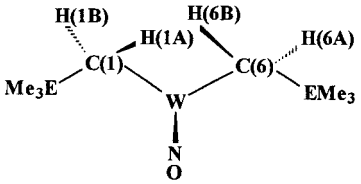

Cp*W(NO)(CH_2CMe_3)$_2$ (**1**)[b]				Cp*W(NO)(CH_2SiMe_3)$_2$ (**2**)		CpW(NO)(CH_2SiMe_3)$_2$ (**3**)			
				Bond Distances (Å)					
W(1)−C(1)	**2.110(3)** 2.106(4)	W(1)−C(6)	**2.175(3)** 2.164(3)	W(1)−C(1)	2.146(5)	W(1)−C(1)	2.103(9)	W(1)−C(6)	2.108(9)
W(1)−H(1A)	**2.233(6)** 2.28(6)	W(1)−H(6A)	**2.745(6)** 2.67(5)	W(1)−H(1A)	2.34(6)				
W(1)−H(1B)	**2.693(6)** 2.56(5)	W(1)−H(6B)	**2.582(6)** 2.46(5)	W(1)−H(1B)	2.60(5)				
C(1)−H(1A)	**1.153(6)** 0.92(6)	C(6)−H(6A)	**1.094(6)** 1.03(5)	C(1)−H(1A)	0.77(6)	C(1)−H	0.98[c]	C(6)−H	0.98[c]
C(1)−H(1B)	**1.070(8)** 0.96(5)	C(6)−H(6B)	**1.083(7)** 0.91(5)	C(1)−H(1B)	0.93(5)				
				Bond Angles (deg)					
W(1)−C(1)−C(2)	**133.4(2)** 133.7(3)	W(1)−C(6)−C(7)	**125.4(2)** 126.2(2)	W(1)−C(1)−Si(1)	124.6(3)	W(1)−C(1)−Si	125.5(5)	W(1)−C(6)−Si	127.1(5)
W(1)−C(1)−H(1A)	**80.6(3)** 88(4)	W(1)−C(6)−H(6A)	**109.7(3)** 108(3)	W(1)−C(1)−H(1A)	95(4)				
W(1)−C(1)−H(1B)	**111.5(3)** 108(3)	W(1)−C(6)−H(6B)	**99.3(3)** 98(3)	W(1)−C(1)−H(1B)	109(3)				
H(1A)-C(1)−H(1B)	**103.9(5)** 101(4)	H(6A)−C(6)−H(6B)	**103.6(5)** 100(4)	H(1A)−C(1)−H(1B)	113(5)				

[a] The Cp′ ligands behind W have been omitted for clarity. [b] Neutron values in boldface type; X-ray values in Roman type. [c] H atoms fixed in idealized positions.

of the UBC mass spectrometry facility using a Kratos MS-50 spectrometer. NMR spectra were obtained at room temperature, unless otherwise noted, on a Varian XL-300 or a Bruker AVA-300, AVA-400, WH-400, or AMX-500 spectrometer. When necessary, selective standard NMR experiments were carried out to correlate and assign ^{1}H and ^{13}C signals. ^{1}H and ^{13}C chemical shifts are recorded in ppm units relative to the residual proton or natural-abundance carbon signal(s) of the solvent employed. ^{2}H{^{1}H} NMR signals are referenced to C_6H_5D (δ 7.15). For brevity, the complete ^{1}H NMR data of the known complexes are not presented again in this paper, since they do not differ from those reported in the literature and they are not required for the establishment of agostic interactions in these complexes. On the other hand, the complete room-temperature gated ^{13}C NMR data for all the complexes are required for an internally consistent assignment of C−H coupling constants; these data have not been reported previously and are therefore presented in Table 4. The simplified NMR signals reflecting only contributions from the α-proton and α-carbon atoms of each complex are specifically listed in Table 3. The measured coupling constants are given in Hz with an estimated experimental error of ±2 Hz in J_{CH} and ±0.5 Hz in J_{HH}.

Improved Preparation of Cp*W(NO)(CH_2CMe_3)$_2$ (1). To a Schlenk flask containing a mixture of Cp*W(NO)Cl_2 (909 mg, 2.16 mmol) and (Me_3CCH_2)$_2$Mg·*x*(dioxane) (277 mg, 2.16 mmol) at −196 °C was added THF (∼40 mL) by vacuum transfer. The resulting brown mixture was thawed and stirred at ∼10 °C for 20 min, during which time it became a dark purple solution. THF was then removed in vacuo, and the flask was returned to the glovebox, charged with additional (Me_3CCH_2)$_2$Mg·*x*(dioxane) (277 mg, 2.16 mmol), and reconnected to a high-vacuum line. Et_2O was then added by vacuum transfer at −196 °C. The resulting mixture was thawed and stirred at room temperature for 30 min, during which time a red solution containing a pale yellow precipitate formed. Next, the solvent was removed in vacuo, and the residue was extracted with 5:1 hexanes/Et_2O (30 mL). The extracts were filtered through alumina I (3 × 2 cm) supported on a medium-porosity frit. The alumina column was washed with additional 5:1 hexanes/Et_2O until the filtrate was colorless. Diminishing the volume of the combined filtrates under reduced pressure, followed by cooling to −30 °C for 2 days, afforded **1** (684 mg, 65% yield in three crops) as dark wine red needles. Crystals of **1** suitable for diffraction analyses were grown by slow cooling of concentrated hexanes solutions. Anal. Calcd for $C_{20}H_{37}NOW$: C, 48.89; H, 7.59; N, 2.85. Found: C, 48.63; H, 7.73; N, 2.77.

Preparation of Cp*W(NO)(CH_2CMe_3)(CD_2CMe_3) (1-*d*$_2$). This complex was prepared in the same manner as described for the synthesis of **1**, except that (Me_3CCD_2)Mg·*x*(dioxane) was used for the second alkylation step. The hexanes/Et_2O extracts were filtered through a pad of Celite rather than alumina I. MS (LREI, *m*/*z*): 493 [M^+, ^{184}W]. IR (cm^{-1}, Nujol): no reduced ν_{C_a-H} observed. Gated ^{13}C{^{1}H} NMR spectra obtained at −80 and +20 °C were identical with that of **1** at +20 °C.

Preparation of Cp*W(NO)(CH_2CMe_3)(NMe_2) (11). To a degassed J. Young NMR tube containing Cp*W(NO)-(CH_2CMe_3)$_2$ (50 mg, 0.10 mmol) was added THF (∼0.5 mL) by vacuum transfer, followed by an excess of Me_2NH (∼10 equiv) via a calibrated bulb attached to a manometer line. The resulting contents were thawed and then heated at ∼75 °C for 2 days, during which time they changed color from wine red to orange. The organic volatiles were removed in vacuo. The residue was extracted with pentane (5 mL), and the mixture was filtered through Celite. To the filtrate was added ∼1 mL of Et_2O. The volume of the resulting solution was then reduced in vacuo, and it was stored at −30 °C overnight to induce the deposition of **11** as yellow-orange needles (43 mg, 93% yield). Anal. Calcd for $C_{17}H_{32}N_2OW$: C, 43.97; H, 6.95; N, 6.03. Found: C, 43.89; H, 7.09; N, 5.91. IR (cm^{-1}): 1566 (s, ν_{NO}). MS (LREI, *m*/*z*, probe temperature 150 °C): 464 [P^+, ^{184}W]. ^{1}H NMR (500 MHz, C_6D_6): δ 0.87 and 1.01 (AB quartet, $^2J_{HH}$ = 13.5, 2H, WCH_2), 1.37 (s, 9H, CMe_3), 1.65 (s, 15H, C_5Me_5), 2.59 (s, 3H, NMe), 3.71 (s, 3H, NMe).

Neutron Diffraction Analysis of Cp*W(NO)(CH_2CMe_3)$_2$ (1). Neutron diffraction data were collected on a single crystal

Table 3. Pertinent α-Proton and α-Carbon NMR Data for Complexes 1−11

				^{1}H[a]						^{13}C[b]			
				R			R′			R		R′	
no.	Cp′M	R	R′	δ(H) (mult, $^2J_{HH}$, $^4J_{HH}$, $^2J_{HW}$)	δ(H) (mult, $^2J_{HH}$)	Δ(δ(H))	δ(H) (mult, $^2J_{HH}$, $^4J_{HH}$, $^2J_{HW}$)	δ(H) (mult, $^2J_{HH}$)	Δ(δ(H))	δ(C) (mult, $^1J_{CH}$, $^1J_{CH}$)	Δ($^1J_{CH}$)	δ(C) (mult, $^1J_{CH}$, $^1J_{CH}$)	Δ($^1J_{CH}$)
1	Cp*W	CH_2CMe_3	CH_2CMe_3	−1.43 (dd, 12.5, 3.5, 11.1)	2.74 (d, 12.5)	4.17				95.3 (dd, 99, 122)	23		
2	Cp*W	CH_2SiMe_3	CH_2SiMe_3	−1.47 (d, 11.1, 8.0)	1.54 (d, 11.1)	3.01				62.7 (dd, 100, 117)	17		
3	CpW	CH_2SiMe_3	CH_2SiMe_3	−0.56 (d, 8.4)[c]	2.23 (d 8.4)	2.79				60.8 (dd, 104, 118)	14		
4	CpMo	CH_2SiMe_3	CH_2SiMe_3	−0.31[d,e] (d, 8.4)[c]	3.02 (d, 8.4)	3.33				66.0[f] (dd, 105, 120)	15		
5	CpW	CH_2CMe_3	CH_2CMe_3	−1.54 (dd, 11.4, 3.5, 8.0)	3.58 (d, 11.4)	5.12				91.4 (dd, 100, 124)	24		
6	CpW	CH_2CMe_2Ph	CH_2CMe_2Ph	−0.98 (dd, 11.1, 3.0)[c]	3.66 (d, 11.1)	4.63				93.8 (dd, 103, 124)	21		
7	Cp*W	CH_2CMe_3	CH_2SiMe_3	−2.12 (dd, 12.8, 1.9, 10.9)	3.28 (d, 12.8)	5.40	−1.29 (dd, 12.0, 2.2, 10.9)	1.07 (d, 12.0)	2.36	106.0 (dd, 94, 123)	29	51.1 (dd, 101,114)	11
8[g]	Cp*W	CH_2CMe_3	Ph	−2.02[e] (d, 11.4)[c]	4.50 (d, 11.4)	6.55				124.9 (dd, 87, 124)	37	181.0 (s)	
9[g]	Cp*W	CH_2CMe_3	CH_2Ph	−2.37[e] (d, 13.2)[c]	2.19 (d, 13.2)	4.56	2.22 (d, 8.4)	2.98 (d, 8.4)	0.76	89.6[f] (dd, 101, 124)	27	52.2 (dd, 132, 137)	5
										60.8[f,h] (pseudo t, ∼115)	<5	44.9 (t, 142)	0
10	Cp*W	CH_2CMe_3	Cl	−0.32 (d, 13.2, 11.4)	3.36 (d, 13.2)	3.68				96.7 (dd, 98, 128)	30		
11	Cp*W	CH_2CMe_3	NMe_2	0.87 (d, 13.5)	1.00 (d, 13.5)	0.13				57.7 (t, 118)	0		

[a] Recorded in C_6D_6 at room temperature at 500 MHz unless otherwise noted. [b] From gated $^{13}C\{^1H\}$ recorded in C_6D_6 at room temperature at 75 MHz unless otherwise noted. [c] J_{HW} not resolved. [d] Recorded at 400 MHz. [f] Recorded at 100 MHz. [g] In CD_2Cl_2. [h] At −80 °C.

Table 4. Room-Temperature Gated ^{13}C NMR Data (δ in ppm and J in Hz) in C_6D_6 at 75 MHz, unless Otherwise Specified

no.	gated ^{13}C NMR data
1	9.9 (q, $^1J_{CH}$ = 128, C_5Me_5), 34.7 (qm, $^1J_{CH}$ = 124, $^3J_{CH}$ = 4.0, CMe_3), 39.2 (m, $^2J_{CH}$ = 3.7, CMe$_3$), 95.3 (ddm, $^1J_{CH}$ = 99, $^1J_{CH}$ = 122, $^3J_{CH}$ = 4.3, CH_2), 110.2 (s, $^3J_{CH}$ = 3.4, C_5Me$_5$)
2	2.9 (q, $^1J_{CH}$ = 117, SiMe$_3$), 9.9 (q, $^1J_{CH}$ = 127, C_5Me_5), 62.7 (dd, $^1J_{CH}$ = 100, $^1J_{CH}$ = 117, CH_2), 110.2 (s, C_5Me$_5$)
3	2.8 (q, $^1J_{CH}$ = 118, SiMe$_3$), 60.8 (dd, $^1J_{CH}$ = 104, $^1J_{CH}$ = 118, CH_2), 101.5 (d, $^1J_{CH}$ = 178, $^2J_{CH}$ = 6.5, C_5H_5)
4[a]	2.5 (q, $^1J_{CH}$ = 118, SiMe$_3$), 66.0 (dd, $^1J_{CH}$ = 104, $^1J_{CH}$ = 120, CH_2), 101.4 (dm, $^1J_{CH}$ = 176, $^2J_{CH}$ = 6.6, C_5H_5)
5	34.3 (qm, $^1J_{CH}$ = 124, $^3J_{CH}$ = 4.5, CMe_3), 39.4 (m, $^2J_{CH}$ = 3.5, CMe$_3$), 91.4 (ddm, $^1J_{CH}$ = 100, $^1J_{CH}$ = 124, $^3J_{CH}$ = 5.2, CH_2), 101.2 (dm, $^1J_{CH}$ = 178, $^2J_{CH}$ = 3.2, C_5H_5)
6	32.7, 33.5 (qm, $^1J_{CH}$ = 124, $^3J_{CH}$ = 4.5, CMeMe), 46.1 (s, CMe$_2$), 93.8 (ddm, $^1J_{CH}$ = 103, $^1J_{CH}$ = 124, $^3J_{CH}$ = 4.9, CH_2), 101.4 (d, $^1J_{CH}$ = 178, $^2J_{CH}$ = 6.6, C_5H_5), 125.6 (dt, $^1J_{CH}$ = 159, $^2J_{CH}$ = 7.8, Ar CH), 126.0 (dt, $^1J_{CH}$ = 156, $^2J_{CH}$ = 7.0, Ar CH), 128.3 (dd, $^1J_{CH}$ = 158, $^2J_{CH}$ = 7.5, Ar CH), 152.8 (s, C_{ipso})
7	2.8 (q, $^1J_{CH}$ = 117, SiMe$_3$), 9.8 (qm, $^1J_{CH}$ = 127, $^4J_{CH}$ = 4.3, C_5Me_5), 34.2 (q, $^1J_{CH}$ = 124, $^3J_{CH}$ = 4.4, CMe_3), 39.8 (m, $^2J_{CH}$ = 4.4, CMe$_3$), 51.1 (dd, $^1J_{CH}$ = 94, $^1J_{CH}$ = 123, CH_2SiMe$_3$), 106.0 (ddm, $^1J_{CH}$ = 101, $^1J_{CH}$ = 123, $^3J_{CH}$ = 4.9, CH_2CMe$_3$), 109.8 (s, C_5Me$_5$)
8[b]	10.2 (q, $^1J_{CH}$ = 127, C_5Me_5), 33.5 (qm, $^1J_{CH}$ = 124, $^3J_{CH}$ = 4.3, CMe_3), 41.4 (s, CMe$_3$), 111.4 (s, C_5Me$_5$), 124.9 (ddm, $^1J_{CH}$ = 89, $^1J_{CH}$ = 124, $^3J_{CH}$ = 5.5, CH_2CMe$_3$), 127.2 (dt, $^1J_{CH}$ = 158, $^2J_{CH}$ = 7.2, Ar CH), 128.3 (dd, $^1J_{CH}$ = 159, $^2J_{CH}$ = 6.8, Ar CH), 136.9 (dm, $^1J_{CH}$ = 155, $^2J_{CH}$ = 7.4, Ar CH), 181.0 (s, Ar C_{ipso})
9[a,b]	at 20 °C: δ 10.4 (q, $^1J_{CH}$ = 127, C_5Me_5), 33.9 (qm, $^1J_{CH}$ = 123, $^3J_{CH}$ = 4.7, CMe_3), 38.8 (m, $^2J_{CH}$ = 3.7, CMe$_3$), 52.2 (dd, $^1J_{CH}$ = 132, $^1J_{CH}$ = 137, $CH_2C_6H_5$), 89.6 (ddm, $^1J_{CH}$ = 101, $^1J_{CH}$ = 124, $^3J_{CH}$ = 4.3, CH_2CMe$_3$), 109.5 (s, C_5Me$_5$), 127.0 (dt, $^1J_{CH}$ = 158, $^2J_{CH}$ = 6.5, Ar C_p), 129.3 (dt, $^1J_{CH}$ = 158, $^2J_{CH}$ = 7.4, Ar C_o or C_m), 131.6 (dt, $^1J_{CH}$ = 158, $^2J_{CH}$ = 6.6, Ar C_o or C_m), 133.2 (Ar C_{ipso}) at −80 °C: δ 10.2 (q, $^1J_{CH}$ = 127, C_5Me_5), 33.2 (q, $^1J_{CH}$ = 122, CMe_3), 36.4 (s, CMe$_3$), 44.9 (t, $^1J_{CH}$ = 122, $CH_2C_6H_5$), 60.8 (pseudo t, $^1J_{CH} \sim$ 115, CH_2CMe$_3$), 107.8 (s, C_5Me$_5$), 117.2 (s, C_{ipso}), 129.2 (d, $^1J_{CH}$ = 159, C_o or C_m), 129.7 (d, $^1J_{CH}$ = 160, C_p), 133.1 (d, $^1J_{CH}$ = 159, C_o or C_m)
10	9.8 (q, $^1J_{CH}$ = 127, C_5Me_5), 33.7 (qm, $^1J_{CH}$ = 124, $^3J_{CH}$ = 3.7, CMe_3), 39.1 (m, $^2J_{CH}$ = 3.9, CMe$_3$), 96.7 (ddm, $^1J_{CH}$ = 98, $^1J_{CH}$ = 128, $^3J_{CH}$ = 4.8,), 112.6 (m, $^4J_{CH}$ = 2.0, C_5Me$_5$)
11	9.52 (q, $^1J_{CH}$ = 127, C_5Me_5), 34.5 (qm, $^1J_{CH}$ = 123, $^3J_{CH}$ = 4.8, CMe_3), 42.2 (m, $^2J_{CH}$ = 3.8, CMe$_3$), 51.3 (qm, $^1J_{CH}$ = 134, $^4J_{CH}$ = 5.0, NMe$_a$), 57.7 (tm, $^1J_{CH}$ = 118, $^4J_{CH}$ = 4.3, WCH_2), 59.8 (qm, $^1J_{CH}$ = 134, $^3J_{CH}$ = 4.7, NMe$_b$), 109.8 (s, C_5Me$_5$)

[a] Recorded at 100 MHz. [b] In CD_2Cl_2.

of **1** at the Institut Laue-Langevin in Grenoble, France, on instrument D19 using a 4° × 64° area detector.[19] Under an inert atmosphere, a red-brown crystal with approximate dimensions 4.8 × 1.8 × 0.48 mm was mounted inside a thin-walled quartz tube, jammed between two plugs of quartz wool to prevent slippage. It was then placed inside a Displex cryostat and slowly cooled. At around 100 K, the crystal appeared to undergo a reversible phase transition; consequently, the temperature was raised to 120 K for the subsequent data collection. At that temperature the crystal details are as summarized in Table 1. Data were collected with neutrons of wavelength 1.5365(2) Å and were integrated in three dimensions. A total of 4644 reflections were merged to give a final data set of 2940 unique reflections (R_{merge} = 4.6%), which were used in the subsequent structure analysis.

The neutron data set of **1** was phased by the atomic coordinates from a previous X-ray analysis (vide infra) using only the non-hydrogen positions from the earlier work. A series of difference Fourier maps gradually revealed the positions of all the H atoms in the molecule, including the four methylene hydrogens on atoms C(1) and C(6). As was found in the X-ray analysis, one of the two *tert*-butyl groups was disordered. The three methyl groups on atom C(2) exhibited packing disorder and had to be refined as two sets of half-methyls, approximately equally populated and related to each other by a 60° rotation about the C(1)−C(2) bond. Fortunately, however, this disorder had no effect on the atomic positions of the two key methylene groups in the molecule. Exhaustive anisotropic least-squares refinement of the structure resulted in the final agreement factors of $R(F)$ = 5.45% for 2579 reflections with $I > 2\sigma(I)$ and $R(F)$ = 6.33% for all data (2940 reflections).

X-ray Crystallographic Analyses of Cp*W(NO)(CH$_2$CMe$_3$)$_2$ (1) and Cp*W(NO)(CH$_2$SiMe$_3$)$_2$ (2). Data for **1** were collected on a Rigaku/ADSC CCD diffractometer at 173(1) K. The final unit cell parameters for **1** were obtained by least-squares on the setting angles for 10 897 reflections with 2θ = 6.4−56.2°. Data for **2** were collected on the same diffractometer at 253(1) K. This temperature was chosen because crystals of **2** were found to be unstable at 173 K. The final unit cell parameters for **2** were obtained by least squares on the setting angles for 6439 reflections with 2θ = 5.9−55.6°. All data were processed and corrected for Lorentz and polarization effects and absorption (semiempirical, based on symmetry analysis of redundant data). Both structures were solved by direct methods[20] and expanded using Fourier techniques.[21] Final refinements were carried out using SHELXL-97.[22]

The complex molecule **1** is partially disordered, with the atoms of one *tert*-butyl group modeled in two orientations with roughly equivalent populations. All non-hydrogen atoms were refined anisotropically, while all hydrogens other than those in positions α to the metal center were placed in calculated positions. The complex molecule **2** resides on a mirror plane parallel to the *b* axis. Once again, all non-hydrogen atoms were refined anisotropically, while all hydrogens other than those in positions α to the metal center were placed in calculated positions. Selected crystallographic data for both the neutron and X-ray structures of **1** and the X-ray structure of **2** are presented in Table 2.

Results and Discussion

Neutron and X-ray Diffraction Analyses of Cp*W(NO)R$_2$ Complexes (R = CH$_2$CMe$_3$, CH$_2$SiMe$_3$). Definitive proof of the existence of agostic interactions within a molecule requires a neutron diffraction analysis.[1c] Consequently, the solid-state molecular structure of the prototypal complex Cp*W(NO)(CH$_2$CMe$_3$)$_2$ (**1**) has

(19) Thomas, M.; Stansfield, R. F. D.; Berneron, M.; Filhol, A.; Greenwood, G.; Jacobe, J.; Feltin, D.; Mason, S. A. In *Position-Sensitive Detection of Thermal Neutrons*; Convert, P., Forsyth, J. B., Eds.; Academic Press: London, 1983; p 344.

(20) Altomare, A.; Burla, M. C.; Cammalli, G.; Cascarano, M.; Giacovazzo, C.; Guagliardi, A.; Moliterni, A. G. G.; Polidori, G.; Spagna, A. *J. Appl. Crystallogr.* **1999**, *32*, 115.

(21) Beurskens, P. T.; Admiraal, G.; Beurskens, G.; Bosman, W. P.; de Gelder, R.; Israel, R.; Smits, J. M. M. Technical Report of the Crystallography Laboratory; University of Nijmegen, Nijmegen, The Netherlands, 1994.

(22) Sheldrick, G. M. University of Gottingen, Gottingen, Germany, 1997.

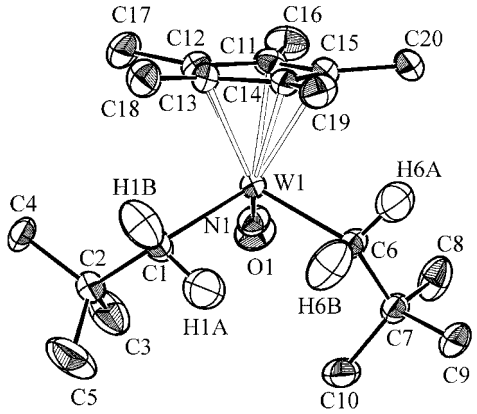

Figure 1. Solid-state molecular structure of Cp*W(NO)-(CH_2CMe_3)$_2$ (**1**), as established by a neutron diffraction analysis at 120 K. Ellipsoids at the 50% probability level are shown. Selected bond lengths (Å) and bond angles (deg): W(1)−N(1) = 1.785(3), N(1)−O(1) = 1.228(3), C(1)−C(2) = 1.538(3), C(6)−C(7) = 1.542(3); W(1)−N(1)−O(1) = 169.1(2), N(1)−W(1)−C(1) = 99.4(2), N(1)−W(1)−C(6) = 99.42(14), C(1)−W(1)−C(6) = 106.48(14).

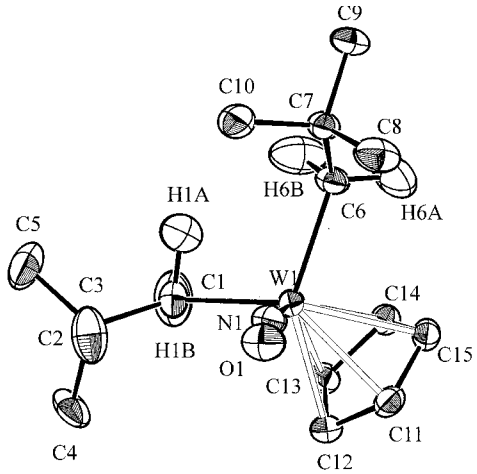

Figure 2. View of the distortion at one of the methylene carbons in the solid-state molecular structure of Cp*W-(NO)(CH_2CMe_3)$_2$ (**1**), as established by a neutron diffraction analysis at 120 K. Ellipsoids at the 50% probability level are shown. Note particularly the acute angle W(1)−C(1)−H(1A) = 80.6(3)°, associated with the "strongly agostic" H(1A) atom.

been established by a neutron diffraction analysis at 120 K, the details of which are summarized in Table 1. This analysis has confirmed the monomeric nature of the complex (Figure 1) and has afforded the intramolecular geometrical parameters presented in Table 2. The Cp*−W and W−NO intramolecular dimensions are generally comparable to those found in related complexes.[9] There is some positional disorder in the ^{t}Bu group of one ligand, perhaps related to a reversible phase change that occurs at lower temperatures. Fortunately, however, this disorder has no effect on the positions of the atoms of the methylene groups, which exhibit the most significant features of the neutron structure. One of the methylene C−H bonds, C(1)−H(1A), is strongly distorted toward the W atom (see Figure 2 and Table 2) in an orientation consistent with interaction between this C−H bond and the vacant metal-based d orbital.[23] The W(1)−C(1)−H(1A) angle associated with this bond (80.6(3)°) is much lower than the normal value (109.5°) expected for an sp^3-hybridized C atom, and the W(1)···H(1A) distance of 2.233(6) Å is in the range anticipated for an agostic interaction. Moreover, the C(1)−H(1A) bond distance of 1.153(6) Å is significantly longer than the other three methylene C−H bonds (average 1.082(7) Å), consistent with a lowering of the C−H bond order. Finally, the W(1)−C(1) bond length and W(1)−C(1)−C(2) bond angle are on the short and wider end of the respective ranges for terminal neopentyl ligands bound to tungsten.[24]

A second notable feature that can be discerned from the neutron results is that another methylene hydrogen, H(6B), appears to be interacting very weakly with the W atom. This interaction is much more subtle; the W(1)−C(6)−H(6B) angle of 99.3(3)° and the W(1)···H(6B) distance of 2.582(6) Å are slightly, but significantly, smaller than expected. Interestingly, the two C−H···W linkages in **1** are approximately coplanar, as the H(1A)−C(1)−W(1) and the H(6B)−C(6)−W(1) planes make angles of 15.0 and 30.6°, respectively, with the C(1)−W(1)−C(6) plane (Figure 1), whereas those in CpNb(=NAr)(CH_2CMe_3)$_2$ are approximately perpendicular to each other.[13] The principal conclusion from the neutron analysis, then, is that in the solid state at 120 K complex **1** possesses one "strongly agostic" (H(1A)) and one "weakly agostic" (H(6B)) methylene hydrogen atom. This unusual "unequal double α-agostic" motif is different from that found for other double α-agostic interactions.[7d,13,25] It could conceivably be a result of intermolecular steric factors, but there are no unusually short contacts involving the packing of the molecules of **1** in the crystal lattice to support such a view.

The X-ray diffraction analysis of **1** at −100 °C (Table 1) has also been performed. Again, there is disorder in one ^{t}Bu group, but all four methylene H's were located and independently refined. For the most part, the solid-state metrical parameters established by the X-ray analysis are fully consistent with those obtained from the neutron study. The W−C bond lengths are short,[24] and the angles around the methylene carbons again indicate the unequal nature of these interactions and confirm that the C(1)−H(1A) link to W is the more distorted of the two. It thus appears that a high-quality, low-temperature X-ray analysis may be sufficient to detect the structural deformations ascribed to agostic interactions. However, the analysis is more qualititative, given the greater estimated standard deviations in the bond lengths associated with the methylene H atoms as compared to those from the neutron analysis (Table 2).

Deformations reflecting α-agostic interactions can also be detected in more symmetrical environments. This feature is illustrated by the X-ray diffraction analysis of Cp*W(NO)(CH_2SiMe_3)$_2$ (**2**) that has been effected at −20 °C (Table 2). This analysis reveals a solid-state

(23) (a) Poli, R.; Smith, K. M. *Organometallics* **2000**, *19*, 2858. (b) Legzdins, P.; Rettig, S. J.; Sánchez, L.; Bursten, B. E.; Gatter, M. G. *J. Am. Chem. Soc.* **1985**, *107*, 1411.

(24) A Cambridge Structural Database search (April 2000 release) reveals a W−C bond length range of 2.076−2.257 Å (median 2.164 Å), and W−C−C angles of 134.75−115.94° (median 124.31°) in 21 compounds.

(25) (a) Mena, M.; Pellinghelli, M. A.; Royo, P.; Serrano, R.; Tiripicchio, A. *J. Chem. Soc., Chem. Commun.* **1986**, *108*, 1118. (b) Bruno, J. W.; Smith, G. M.; Marks, T. J.; Fair, C. K.; Schultz, A. J.; Williams, J. M. *J. Am. Chem. Soc.* **1986**, *108*, 40.

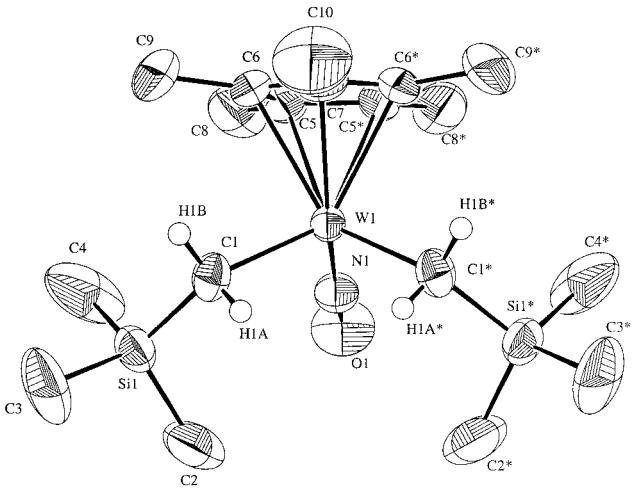

Figure 3. Solid-state molecular structure of Cp*W(NO)-$(CH_2SiMe_3)_2$ (**2**), as established by an X-ray crystallographic analysis at −20 °C. Ellipsoids at the 50% probability level are shown. Selected bond lengths (Å) and bond angles (deg): W(1)−N(1) = 1.745(6), N(1)−O(1) = 1.233(7), C(1)−Si(1) = 1.848(6); W(1)−N(1)−O(1) = 168.4(5), N(1)−W(1)−C(1) = 97.7(2), C(1)−W(1)−C(1)* = 108.2(3).

molecular structure different from that of **1** due to a crystallographically imposed mirror plane (Figure 3). Nevertheless, the methylene H's were located and refined independently, and the resulting W(1)−C(1)−H(1A) angle is acute compared to W(1)−C(1)−H(1B). The W(1)−C(1) bond length is average compared to other terminal W−CH_2SiMe_3 groupings, but the W(1)−C(1)−Si(1) bond angle is large.[26] These structural features indicate either equivalent agostic interactions for each (trimethylsilyl)methyl ligand in **2** or the existence on average of some degree of C−H···M interaction for each CH_2SiMe_3 group.

A comparison of these metrical parameters of **2** with those previously reported for the ambient-temperature structure of its Cp analogue (**3**)[10] suggests the existence of similar agostic interactions in **3**. Thus, even though the methylene hydrogens were not located during the original analysis of **3** but rather were fixed in idealized positions, the W−C−Si angles listed in Table 2 for **3** are more obtuse than those of **2**, and the W−C bond length is shorter.

NMR Spectroscopic Properties of 1. While it is clear that there are α-agostic interactions in the solid-state structures of **1** and its Si-containing analogues **2** and **3**, it remains to be determined whether these interactions persist in solutions. Two spectral features are indicative of α-agostic interactions in the solution structure of a compound,[1b] namely (1) a large chemical-shift difference between methylene proton signals in the ^{1}H NMR spectrum, with one resonance appearing below 0 ppm, and (2) unequal $^1J_{CH}$ values for the α-carbon in the gated-decoupled ^{13}C NMR spectrum, with one being significantly reduced when compared to normal values. As previously reported, the ^{1}H NMR spectrum of **1** exhibits the first of these features, namely two chemically inequivalent methylene proton signals at 2.74 ppm

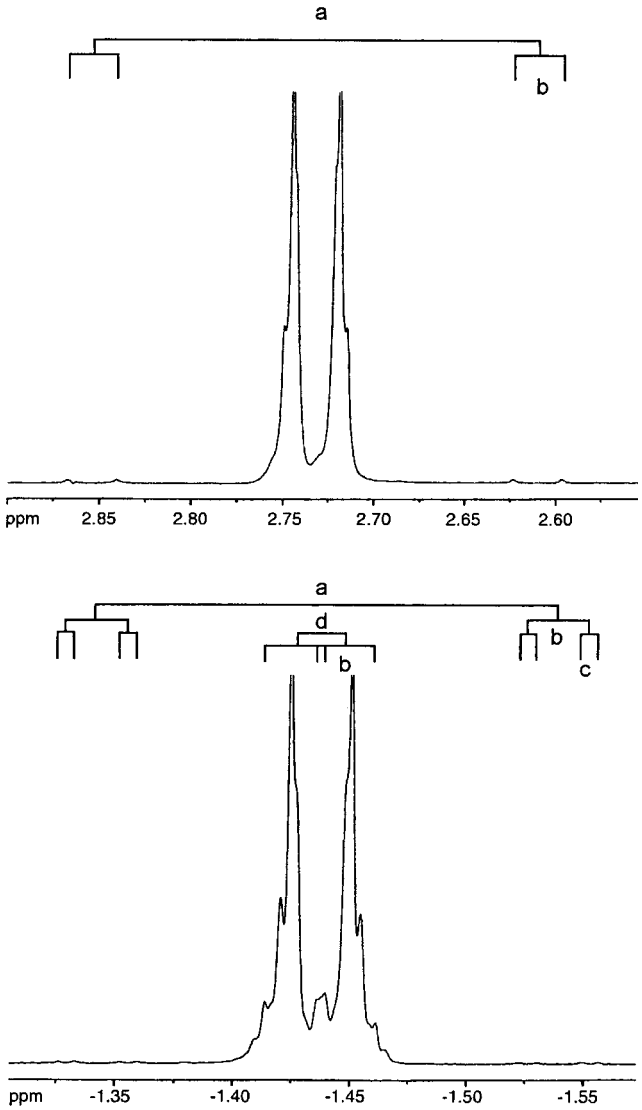

Figure 4. Portions of the 500 MHz ^{1}H NMR spectrum of **1** in C_6D_6, showing the resonances attributable to the methylene hydrogen atoms. The indicated coupling constants are as follows: (a) $^1J_{CH}$; (b) $^2J_{HH}$; (c) $^4J_{HH}$; (d) $^2J_{HW}$.

and, most notably, −1.43 ppm (Table 3).[16] The newly recorded partial high-field spectrum of **1** also reveals a second-order coupling, as shown in Figure 4. The AA′BB′ pattern is overlaid on an AA′BB′X pattern, where X = ^{183}W, ca. 14% abundant, with the upfield resonance being strongly coupled to ^{183}W ($^2J_{HW}$ = 11.1 Hz). These features clearly indicate that the upfield methylene proton is interacting with the metal center, consistent with an agostic interaction involving the innermost methylene H atom of the neopentyl ligand and the metal center as occurs in the solid-state structure (vide supra). Similar second-order coupling patterns have been reported for the isostructural dialkyl alkylidyne complexes CpW(CR)R′$_2$, which also exhibit α-agostic interactions between the metal center and the innermost, upfield protons.[7d]

Consistent with the features of the proton spectrum, the gated ^{13}C{^{1}H} NMR spectrum of **1** reveals that the α-carbon ^{13}C resonance is split into a doublet of doublets by two different $^1J_{CH}$ values of 99 and 122 Hz. The doublet of doublets is further split by long-range coupling to the methyl H's of the neopentyl group and the

(26) A Cambridge Structural Database search (April 2000 release) reveals a W−C bond length range of 2.042−2.285 Å (median 2.141 Å), and W−C−Si angles of 115.84−132.95° (median 120.75°) in 35 compounds.

Cp* ligand ($^3J_{CH} \approx 4.5$ Hz, Table 4). The ^{13}C satellites in the ^{1}H NMR spectrum indicate that the smaller $^1J_{CH}$ is associated with the upfield proton resonance, again consistent with the existence of an α-agostic interaction between the inner methylene proton of the neopentyl ligand and the metal center. Finally, the chemical shift for the α-carbon at ~95 ppm is quite downfield as compared to the α-carbon resonances for other neopentyl ligands in related electronically saturated complexes (vide infra).[16,27] Similar downfield shifts have also been noted for the α-carbon resonances of alkylidene ligands in isostructural complexes as the degree of α-agostic interaction increases.[7b,28]

Unlike the solid-state structure of **1**, in which there is one strongly and one weakly interacting agostic methylene C−H bond, the solution spectroscopic data seem to indicate the presence of two equivalent agostic interactions on the NMR time scale. These interactions could be static, in which case the structural motif is different. Alternatively, the interactions could be dynamic in nature, in which case the observed symmetry is reflective of an average picture of the molecule in solution. Attempts were made to resolve this issue by using variable-temperature NMR spectroscopy. However, the gated ^{13}C{^{1}H} NMR spectra of **1** in toluene-d_8 exhibit no significant changes (i.e., within experimental error) in the coupling constants from 301 to 193 K. Likewise, no significant spectral changes occur for the α-carbon ^{13}C resonance in the partially deuterated complex Cp*W(NO)(CH$_2$CMe$_3$)(CD$_2$CMe$_3$) (**1**-d_2) under the same conditions. Hence, no conclusion concerning the static or dynamic nature of the coordination of the C−H(D) bonds to the W center can be drawn. Nevertheless, given the solid-state structure of **1** as well as the solution results for other congeners (vide infra), we believe that the system is probably dynamic. Thus, the limiting solution structures of **1** and **1**-d_2 each contain one strongly agostic and one weakly agostic neopentyl ligand. A rapid exchange of agostic bonding forms would then afford the observed time-averaged NMR spectra even at −80 °C, i.e.

W = Cp*W(NO)

NMR Spectroscopic Properties of Cp*W(NO)(R)(R′) (R′ = Alkyl, Aryl, Benzyl, Halidee, Amide) Complexes. The crystallographic and spectroscopic studies described in the preceding paragraphs clearly establish the existence of agostic interactions in **1** both in solution and in the solid state. We next explored the factors influencing agostic interactions in the solution structures of related nitrosyl compounds, namely the symmetric dialkyl complexes **2**−**6**, the mixed hydrocarbyls **7**−**9**, and the Cp*W(NO)(CH$_2$Me$_3$)(X) (X = π-donor) complexes **10** and **11**. The pertinent ^{1}H and gated ^{13}C{^{1}H} NMR spectral parameters of the α-H and α-C atoms for **1**−**11** are collected in Table 3. Notable features of the data in this table include the following.

(1) The room-temperature ^{1}H and ^{13}C NMR spectral features of the symmetric dialkyls **2**−**6** are similar to those of Cp*W(NO)(CH$_2$CMe$_3$)$_2$ (**1**) discussed above. Each symmetry-related WCH$_2$E (E = CMe$_3$, SiMe$_3$, CMe$_2$Ph) group exhibits two ^{1}H resonances due to the chemically inequivalent methylene protons. The second-order nature of the methylene proton resonances is only resolvable for the neopentyl ligands in **5**, which also has the upfield resonance more strongly coupled to ^{183}W ($^2J_{HW}$ = 8.0 Hz). The geminal α-hydrogens in each WCH$_2$E group in **2**−**6** are coupled to the corresponding alkyl α-carbon atom to a different extent. Consequently, each W*C*H$_2$E ^{13}C resonance is split into a doublet of doublets by one $^1J_{CH}$ in the range 117−124 Hz and the other in the range of 99−104 Hz (Table 3) (with fine coupling observed for E = CMe$_3$, CMe$_2$Ph; see Table 4). In all instances, the reduced $^1J_{CH}$ is associated with the upfield methylene proton signals, as judged from the ^{13}C satellites in the ^{1}H NMR spectra. Finally, the chemical shifts for the α-carbon signals of each alkyl ligand are downfield from those found in isostructural electronically saturated complexes bearing the same ligands.[10,24,29]

A comparison of these data for **1**−**6** reveals similar spectral properties despite changes to the metal center, the alkyl ligands, and the Cp′ ligand. It thus appears that α-agostic interactions are common in solution for all *symmetric dialkyl* complexes of the general type Cp′M(NO)R$_2$ (M = Mo, W) and that these complexes should therefore be regarded as possessing greater than 16-valence-electron ground-state configurations. It should also be noted that the magnitude of the differences in chemical shift (Δ(δ(H)) and coupling constant (Δ($^1J_{CH}$)) appear to depend on the nature of the hydrocarbyl ligand (i.e., E = CMe$_3$ ≈ CMe$_2$Ph > SiMe$_3$).

(2) Complexes **7**−**9** are chiral mixed hydrocarbyl complexes. Consequently, they show not only separate NMR signals for each of the α-carbons and associated α-methylene protons but also different splitting patterns for the latter, depending upon the nature of R and R′ (Table 3). For the mixed-alkyl complex **7**, resonances for two independent methylene groups occur in the ^{1}H and gated ^{13}C{^{1}H} NMR spectra. NOE and HMQC experiments have been conducted to establish the stereochemical relationship of the α-methylene protons in solution. These experiments revealed that the most and least upfield protons are associated with the neopentyl ligand, as assigned in Table 3. Also, the protons that give rise to the upfield doublets of doublets for each ligand are in close proximity to each other. This observation is consistent with **7** having a limiting solution structure similar to the solid-state structure of **1** with the inner C−H bonds of *both* its alkyl ligands interacting with the metal center in solution. Interestingly, the neopentyl ligand shows a larger chemical shift difference, a larger difference in $^1J_{CH}$, and a higher α-carbon ^{13}C chemical shift than the neopentyl ligands in the symmetric congener **1.** Moreover, the (trimethylsilyl)methyl ligand exhibits lower values compared to the neopentyl ligand in **7** as well as in the bis((tri-

(27) (a) Legzdins, P.; Phillips, E. C.; Sánchez, L. *Organometallics* **1989**, *8*, 940. (b) Legzdins, P.; Lundmark, P. J.; Phillips, E. C.; Rettig, S. J.; Veltheer, J. E. *Organometallics* **1992**, *11*, 2991.

(28) (a) Nugent, W. A.; Mayer, J. M. *Metal−Ligand Multiple Bonds*; Wiley: New York, 1988; Chapter 4.

(29) Debad, J. D.; Legzdins, P.; Lumb, S. A. *Organometallics* **1995**, *14*, 2543.

methylsilyl)methyl) congener **2**. These spectral features could arise from competitive and unequal agostic interactions in **7**, with the neopentyl ligand being "more agostic" in solution; i.e., on average there is a preference for the interaction between the methylene C−H bond of the neopentyl ligand and the metal center over that involving the (trimethylsilyl)methyl ligand. A VT gated $^{13}C\{^1H\}$ NMR study of **7** in toluene-d_8 from 301 to 193 K again shows no significant changes in the $^1J_{CH}$ values. Hence, these unequal interactions are either static or, most likely, dynamic on the NMR time scale (vide infra) with very modest differences in energy between the dominant neopentyl agostic and the dominant (trimethylsilyl)methyl agostic forms.

W = Cp*W(NO)

It is possible that other structural differences in **1**, **2**, and **7** contribute to, or are solely responsible for, the observed spectral differences between the neopentyl and the (trimethylsilyl)methyl ligands, independent of the interaction of the methylene C−H bonds with the metal center.[30] However, the representative alkyl aryl complex **8** exhibits more pronounced spectral distortions for the neopentyl ligand: namely, larger chemical shift and $^1J_{CH}$ differences than **7**, as well as a higher field α-carbon resonance. Consequently, we believe that these spectral features are most consistent with there being a more α-agostic neopentyl ligand in **8** than in **1** resulting from the absence of a competitive α-agostic interaction from the aryl ligand.

The spectroscopic data for the representative benzyl complex **9** are more complicated but provide credibility to the spectral interpretations proffered for **1**−**8**. At room temperature, the neopentyl methylene carbon and protons give rise to signals (Table 3) indicative of a modest agostic interaction involving this ligand. However, the NMR signals for the methylene protons of the benzyl ligand in this compound are intermediate between those exhibited by η^1-benzyl (δ 0−1, $^2J_{HH} \approx 10$ Hz) and η^2-benzyl (δ 2−3, $^2J_{HH} \approx 5-7$ Hz) ligands.[15,31] The same feature is also evident for the ipso and methylene carbon resonances (Table 3). These data can be rationalized in terms of an equilibrium in which the neopentyl and benzyl ligands of **11** are rapidly exchanging their modes of attachment to the tungsten center at room temperature; i.e.

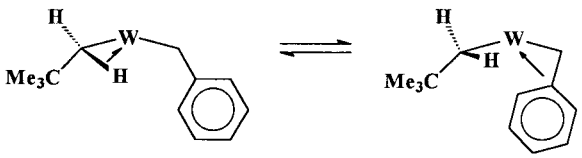

W = Cp*W(NO)

Consistent with this view is the fact that the NMR spectra of **9** are temperature-dependent. Cooling a sample of **9** in CD_2Cl_2 to −80 °C causes the gated $^{13}C\{^1H\}$ NMR spectrum to change in the following manner. First, the signal due to the neopentyl methylene carbon shifts upfield by ca. 30 ppm while its $^1J_{CH}$ coupling constant increases to ca. 115 Hz, a value that is more characteristic of a nonagostic neopentyl ligand. Second, the signals for both the benzyl methylene (δ 44.9) and benzyl ipso (δ 117.2) carbons are similarly shifted to lower frequencies. Importantly, the chemical shift of the latter is to the region associated with static η^2-benzyl ligands, while the $^1J_{CH}$ coupling constant (142 Hz) for the former is consistent with there being considerable sp^2 character at this carbon.[1b,15] On the basis of these observations it can be concluded that (1) the low-temperature limiting structure for **9** is one in which the benzyl ligand is coordinated to tungsten in an η^2 fashion and the neopentyl ligand is nonagostic and (2) at room temperature this η^2-benzyl−metal interaction is fluxional and interconverts with its η^1 form, thereby allowing an α-C−H bond of the neopentyl ligand to compete for coordination to the metal center. Moreover, the stereochemical nonrigidity of **9** lends credence to the interpretation that **1**−**8** also possess competitive and dynamic α-agostic interactions in solution.

(3) The last two complexes in Table 3, namely **10** and **11**, contain a potential π-donating ligand in addition to the neopentyl ligand. The ^1H and ^{13}C NMR spectra of the chloro complex **10** display methylene signals with chemical shifts and coupling constants ($\Delta\delta_{HH} = 3.68$ ppm, $^1J_{CH} = 98$, 128 Hz) indicative of an α-agostic neopentyl ligand. The presence of lone-pair electrons on the chloro ligand thus appears to have no significant effect on the ability of the neopentyl to form a three-center, two-electron bond with tungsten in **10**. A similar lack of effects by Cl ligands has been reported for the α-agostic complexes $(dmpe)(Cl)_3Ti(CH_3)$[32] and Tp*Nb(Cl)(R)(PhC≡CMe) (R = CH_3, CH_2CH_3, CH_2SiMe_3).[33]

Finally, in contrast to the NMR spectra of complexes **1**−**10**, the NMR spectra of the neopentyl complex Cp*W(NO)(CH_2CMe_3)(NMe_2) (**11**) display normal chemical shifts and coupling constants for the α-methylene protons and carbons. The $^1J_{CH}$ value of 118 Hz for **11**, in particular, is indicative of a nonagostic structure for this compound. In the ^1H NMR spectrum of **11**, the methyl substituents of the NMe_2 ligand give rise to two sharp singlets at δ 2.59 and 3.71, which remain unchanged even when the sample is heated to 100 °C. This observation suggests that the amido ligand is functioning as a strong π-donor to the W center. The lack of agostic interactions in this complex can therefore be attributed to the inability of an α-C−H bond on the neopentyl group to compete with the lone pair of electrons on N for coordination to the metal. Similar effects of strong π-donors on agostic interactions have been observed in several other systems.[7d,34]

Chemical Consequences of α-Agostic Interactions in Cp*W(NO)(R)(R′) Complexes. The picture

(30) (a) Xue, Z.; Liting, Li; Lenore, K. H.; Diminnie, J. B.; Pollitte, J. L. *J. Am. Chem. Soc.* **1994**, *116*, 2169. (b) Finch, W. C.; Anslyn, E. V.; Grubbs, R. H. *J. Am. Chem. Soc.* **1988**, *110*, 2406.

(31) Legzdins, P.; Jones, R. H.; Phillips, E. C.; Yee, V. C.; Trotter, J.; Einstein, F. W. B. *Organometallics* **1991**, *10*, 1002.

(32) Dawoodi, Z.; Green, M. L. H.; Mtetwa, V. S. B.; Prout, K.; Schultz, A. J.; Williams, J. M.; Koetzle, T. F. *J. Chem. Soc., Dalton Trans.* **1986**, 1629.

(33) Etienne, M.; Mathieu, R.; Donnadieu, B. *J. Am. Chem. Soc.* **1997**, *119*, 3218.

(34) (a) Etienne, M. *Organometallics* **1994**, *13*, 410. (b) Boncella, J. M.; Cajigal, M. L.; Abboud, K. A. *Organometallics* **1996**, *15*, 1905.

that has emerged from these investigations is that complexes of the type Cp*W(NO)(R)(R′) do adopt an α-agostic structure both in solution and in the solid state when secondary interactions such as π-electron donation are weak (**10**), competitive (**9**), or not possible (**1**−**8**). Moreover, density-functional theoretical calculations by Poli and Smith have shown that the α-agostic interactions in $CpW(NO)Me_2$ are geometric precursors to facile cleavage of the α-H bond by a metal-assisted abstraction pathway.[23a] This suggests that the presence or absence of α-agostic interactions in **1**−**11** could drastically affect their ability to undergo α-H abstractions.

However, the actual chemical consequences of these interactions with respect to α-H cleavage reactions are somewhat surprising. Kinetic studies of the rate of neopentane elimination from complexes **1** and **9** in benzene-d_6 have shown that the rates are very similar ($k_{\mathbf{1}} = [4.6(1)] \times 10^{-5}$ s^{-1} and $k_{\mathbf{9}} = [4.9(1)] \times 10^{-5}$ s^{-1} at 72.0 °C; $k_{\mathbf{9}}/k_{\mathbf{1}} = 1.07$).[11b] This is so despite the fact that **1** has a weakened α-C−H bond in its average agostic solution structure, whereas **9** would have to lose its agostic neopentyl C−H bond in order to attain the transition state for α-H abstraction from its benzyl ligand. This apparent lack of influence of α-C−H···M bonding on the energy required for C−H bond cleavage is in sharp contrast to the related $CpW(\equiv CR)(CH_2R')_2$ (R, R′ = CMe_3, 1-adamantyl) systems, in which the rate of α-H atom migration has been linked to the presence of α-agostic interactions in the ground state.[7d]

Similarly, complex **7** is thermally robust and undergoes α-H neopentane elimination only very slowly (i.e., ca. 5% decomposition over 40 h at 70 °C in TMS).[11b] Furthermore, complex **8**, which in solution appears to have a more distorted α-agostic neopentyl ligand than **1**, does not form the neopentylidene complex Cp*W(NO)(=$CHCMe_3$), when thermolyzed in benzene-d_6 (as determined by the absence of **8**-d_6 over 40 h at 70 °C). Instead, **8** undergoes β-H elimination of neopentane to form a benzyne complex and ultimately Cp*W(NO)(C_6H_4D)(C_6D_5) at a rate significantly slower than alkylidene formation from **1** and **9**.[35] These observations are not in accord with the concept that α-agostic alkyl ligands are incipient alkylidene ligands.[7d,36]

Clearly, the α-agostic interactions in the ground-state structures of complexes **1**, **7**, **8**, and **9** do not significantly influence the pathway and the rate of thermal decomposition. Other steric and electronic factors, such as the bond strengths of the M−C and C−H bonds being broken and formed in the α- or β-H atom transfers, must therefore be responsible for the observed thermal properties of these complexes.

Acknowledgment. R.B. thanks the U.S. National Science Foundation and the American Chemical Society for financial support and acknowledges Thomas F. Koetzle, Arthur J. Schultz, Manfred Bortz, and Martha Miller in the earlier stages of the neutron diffraction analysis. P.L. is grateful to the Natural Sciences and Engineering Research Council of Canada for support of this work in the form of grants to him and a postgraduate fellowship to C.S.A. W.B.S. also thanks the University of British Columbia for the award of University Graduate Fellowships, and we acknowledge Mr. Trevor W. Hayton for helpful discussions and Ms. Elizabeth Tran for initial investigations in this area.

Supporting Information Available: ORTEP drawings and tables listing crystallographic information, atomic coordinates and B_{eq} values, anisotropic thermal parameters, and intramolecular bond distances, angles, and torsion angles. This material is available free of charge via the Internet at http://pubs.acs.org.

OM0106231

(35) Debad, J. D. Ph.D. Dissertation, University of British Columbia, 1989.

(36) Fellmann, J. D.; Schrock, R. R.; Traficante, D. D. *Organometallics* **1982**, *1*, 481.